

Supporting Information

Direct water-based synthesis and characterization of new Zr/Hf-MOFs with dodecanuclear clusters as IBU

Steve Waitschat,^a Helge Reinsch,^a Merve Arpacioğlu^a and Norbert Stock^a

*^a Institute für Anorganische Chemie, Christian-Albrechts-Universität,
Max-Eyth-Straße 2, D 24118 Kiel, Germany*

Prof. Dr. Norbert Stock, Tel.: +49-431-880-1675, Fax: +49-431-880-1775,
Email: stock@ac.uni-kiel.de

Table of Contents

S1 Methods and Reagents

S2 Synthesis and Characterization of the Linker H₂APDC

S3 Discovery, Optimization and Synthesis of M-CAU-39

**S4 Structural Analysis of M-CAU-39:
Details of Rietveld refinement; Structure; Crystallographic
Tables**

S5 M-CAU-39: Thermal stability

S6 M-CAU-39: IR Spectroscopy

S7 M-CAU-39: N₂ Sorption Experiments

S8 References

S1 Methods and Reagents

Initial characterization was performed using a Stoe Stadi P X-ray diffractometer equipped with a xy-stage, in transmission geometry using Cu $K_{\alpha 1}$ radiation and with data collected by a Mythen detector. Powder X-Ray Diffraction (PXRD) patterns for structure determination were measured using a Stoe Stadi MP diffractometer in transmission geometry using Cu $K_{\alpha 1}$ radiation and with data collected using a Mythen detector. Infrared spectra were recorded on a Bruker ALPHA-P A220/D-01 FTIR spectrometer equipped with an ATR unit, over the spectral range of 4000-40 cm^{-1} . Thermogravimetric analysis was carried out using a NETZSCH STA 429 CD analyzer with a heating rate of 4 K min^{-1} and under flowing air (flow rate 75 ml min^{-1}). Sorption isotherms were measured at -196°C for N_2 and 25°C for H_2O with a BELSORP-max apparatus (BEL Japan Inc.).

Table S1.1. List of reagents used in the synthesis and their suppliers.

Reagent	Supplier	Reagent	Supplier
HfCl_4	ABCR	Formic acid	BASF
$\text{ZrOCl}_2 \cdot 8\text{H}_2\text{O}$	ABCR	Acetic acid	VWR
		Hydrochloric acid	Walter CMP
		Ethanol	Walter CMP

4,4'-azopyridine-dicarboxylic acid (H_2APDC) was synthesized following the method reported by Ameerunisha.¹

Table S1.2. List of reagents and suppliers used in the synthesis of the linker H_2APDC .

Reagent	Supplier	Reagent	Supplier
5-Nitropicolinic acid	ABCR	Sodium hydroxide	Grüssing
Hydrochloric acid	VWR	D-Glucose	Grüssing

S2 Synthesis and Characterization of the Linker H₂APDC

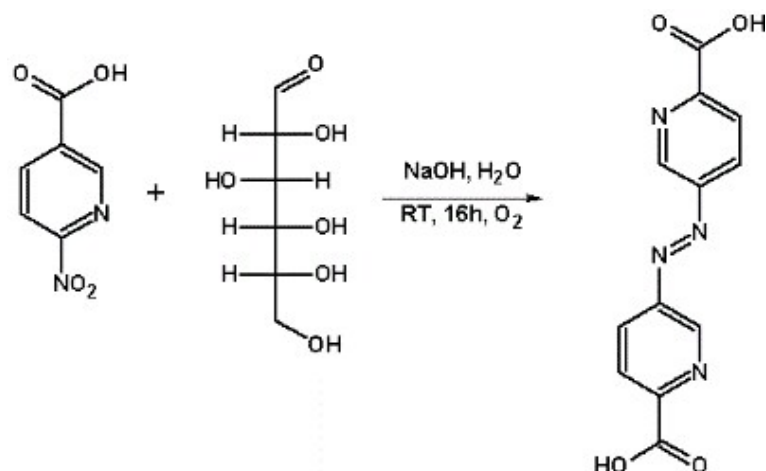


Fig. S2.1: Reaction scheme for the synthesis 4,4'-azopyridine-dicarboxylic acid from 5-nitropicolinic acid.

The synthesis was carried out according to the literature.^[1] 5 g (0.03 mol) 5-nitro-picolinic acid was dissolved in 66 ml H₂O with 13 g (0.325 mol) NaOH in a 250 ml round bottom flask, the mixture was stirred for 1 h at 60 °C. In this time 27 g D-glucose (0.21 mol) was dissolved in 40 ml H₂O at approximately 40 °C. The sugar solution was added to the round bottom flask and the whole synthesis mixture was stirred at 60 °C for 3 h. Afterwards the mixture was cooled down to room temperature and was stirred for 16 h while bubbling pressurized air through the solution. Subsequently the product was filtered off, the solid was dissolved in approximately 200 ml H₂O and precipitated with conc. HCl. The observed red-orange powder was analyzed with ¹H-NMR spectroscopy.

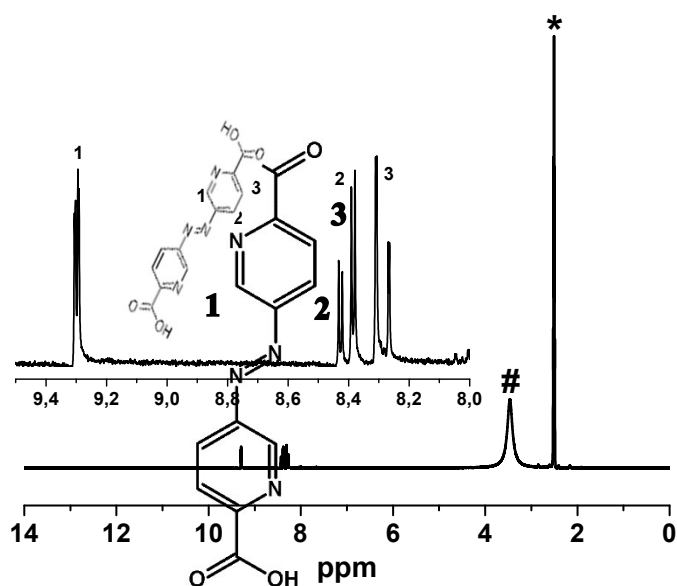


Fig. S2.2: ¹H-NMR spectrum of 4,4'-azopyridine-dicarboxylic acid dissolved in (CD₃)₂SO (* signal of (CD₃)₂SO and # signal of water).

Synthesis and Characterization of M-CAU-39

S3 Discovery, Optimization and Synthesis of M-CAU-39

The systematic investigation of the chemical system $M^{4+}/APDC^{2-}$ of M-CAU-39 with $M = Zr^{4+}$ and Hf^{4+} was carried out via Pyrex-tubes heated up in an aluminum block. The synthesis conditions of CAU-22^[2] were initially used and optimized towards the optimized synthesis conditions of CAU-39. Detailed reaction conditions are summarized in Tab. S3.1 and Tab. S3.2. The optimized reaction conditions are indicated by a red box.

Table S3.1. Reaction parameters of the synthesis optimisation of Zr-CAU-39. $M = ZrOCl_2 \cdot 8H_2O$, The red box shows the optimized reaction parameter for the synthesis of Zr-CAU-39. The metal to linker ratio was fixed to 1:1 for every reaction. Mod = Modulator.

M / g	H ₂ APDC / g	H ₂ O / μ L	Modulator	Mod. / μ L	T / °C	t / min
0.0322	0.0273	400	HCOOH	1600	140	60
0.0322	0.0273	400	HCOOH	1600	140	120
0.0322	0.0273	400	HCOOH	1600	140	180
0.0322	0.0273	400	HCOOH	1600	140	240
0.0322	0.0273	400	CH ₃ COOH	1600	140	5
0.0322	0.0273	400	CH ₃ COOH	1600	140	10
0.0322	0.0273	400	CH ₃ COOH	1600	140	20
0.0322	0.0273	400	CH ₃ COOH	1600	140	30
0.0322	0.0273	400	CH ₃ COOH	1600	140	40
0.0322	0.0273	400	CH ₃ COOH	1600	140	50
0.0322	0.0273	400	CH ₃ COOH	1600	140	60
0.0322	0.0273	400	CH ₃ COOH	1600	140	70
0.0322	0.0273	400	CH ₃ COOH	1600	140	80
0.0322	0.0273	400	CH ₃ COOH	1600	140	90
0.0322	0.0273	400	CH ₃ COOH	1600	140	100
0.0322	0.0273	400	CH ₃ COOH	1600	140	120
0.0322	0.0273	400	CH ₃ COOH	1600	140	180
0.0322	0.0273	400	CH ₃ COOH	1600	160	5
0.0322	0.0273	400	CH ₃ COOH	1600	160	20
0.0322	0.0273	400	CH ₃ COOH	1600	160	60
0.0322	0.0273	400	CH ₃ COOH	1600	160	120
0.0322	0.0273	400	CH ₃ COOH	1600	160	180
0.0161	0.0136	1200	CH ₃ COOH	800	140	5
0.0161	0.0136	1200	CH ₃ COOH	800	140	10
0.0161	0.0136	1200	CH ₃ COOH	800	140	20
0.0161	0.0136	1200	CH ₃ COOH	800	140	30
0.0161	0.0136	1200	CH ₃ COOH	800	140	40
0.0161	0.0136	1200	CH ₃ COOH	800	140	50
0.0322	0.0273	400	C ₂ H ₅ COOH	1600	140	5
0.0322	0.0273	400	C ₂ H ₅ COOH	1600	140	10
0.0322	0.0273	400	C ₂ H ₅ COOH	1600	140	20
0.0322	0.0273	400	C ₂ H ₅ COOH	1600	140	30
0.0322	0.0273	400	C ₂ H ₅ COOH	1600	140	40
0.0322	0.0273	400	C ₂ H ₅ COOH	1600	140	50
0.0322	0.0273	400	C ₂ H ₅ COOH	1600	140	60
0.0322	0.0273	400	HCl	1600	140	5
0.0322	0.0273	400	HCl	1600	140	10
0.0322	0.0273	400	HCl	1600	140	20
0.0322	0.0273	400	HCl	1600	140	30

0.0322	0.0273	400	HCl	1600	140	40
0.0322	0.0273	400	HCl	1600	140	50
0.0322	0.0273	400	HCl	1600	140	60

Table S3.2. Reaction parameters of the synthesis optimisation of Hf-CAU-39. M = HfCl₄. The red box shows the optimized reaction parameter for the synthesis of Hf-CAU-39. The metal to linker ratio was fixed to 1:1 for every reaction. Mod = Modulator.

M / g	H ₂ APDC / g	H ₂ O / μ L	Modulator	Mod. / μ L	T / $^{\circ}$ C	t / min
0.0289	0.0136	1600	HCOOH	400	140	5
0.0289	0.0136	1600	HCOOH	400	140	10
0.0289	0.0136	1600	HCOOH	400	140	20
0.0289	0.0136	1600	HCOOH	400	140	30
0.0289	0.0136	1600	HCOOH	400	140	40
0.0289	0.0136	1600	HCOOH	400	140	50
0.0289	0.0136	1600	HCOOH	400	140	60
0.0289	0.0136	1200	HCOOH	800	140	5
0.0289	0.0136	1200	HCOOH	800	140	10
0.0289	0.0136	1200	HCOOH	800	140	20
0.0289	0.0136	1200	HCOOH	800	140	30
0.0289	0.0136	1200	HCOOH	800	140	40
0.0289	0.0136	1200	HCOOH	800	140	50
0.0289	0.0136	1200	HCOOH	800	140	60
0.0289	0.0136	1600	CH ₃ COOH	400	140	5
0.0289	0.0136	1600	CH ₃ COOH	400	140	10
0.0289	0.0136	1600	CH ₃ COOH	400	140	20
0.0289	0.0136	1600	CH ₃ COOH	400	160	30
0.0289	0.0136	1600	CH ₃ COOH	400	160	40
0.0289	0.0136	1600	CH ₃ COOH	400	160	50
0.0289	0.0136	1600	CH ₃ COOH	400	160	60
0.0289	0.0136	1200	CH ₃ COOH	800	160	5
0.0289	0.0136	1200	CH ₃ COOH	800	140	10
0.0289	0.0136	1200	CH ₃ COOH	800	140	20
0.0289	0.0136	1200	CH ₃ COOH	800	140	30
0.0289	0.0136	1200	CH ₃ COOH	800	140	40
0.0289	0.0136	1200	CH ₃ COOH	800	140	50
0.0289	0.0136	1200	CH ₃ COOH	800	140	60

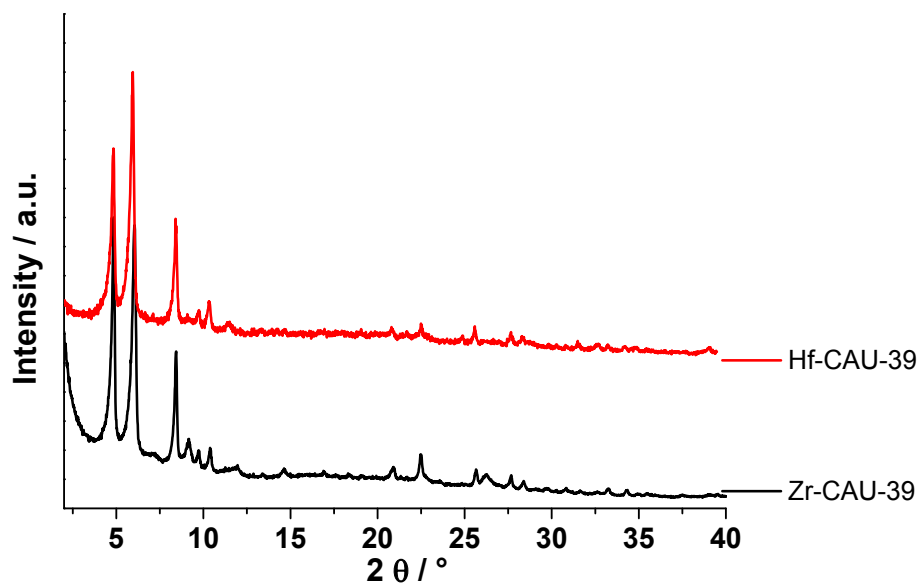


Fig. S3.1: PXRD patterns of the obtained M-CAU-39, with M = Zr, Hf from the optimized reaction conditions.

S4 Structural Analysis of M-CAU-39

S4 Details of the Rietveld Refinement

The PXRD pattern for Hf-CAU-39 was measured in transmission geometry using $\text{CuK}\alpha_1$ radiation and could be successfully indexed using TOPAS academics^[3] with a hexagonal cell with extinction conditions suitable for space group $P6_3/m$. The space group symmetry thus is lower than the one of the recently reported MOF based on biphenyldicarboxylic acid^[4] ($P6_3/mmc$). Still, a suitable model was developed by converting the crystal structure of the former compound using the Materials Studio software.^[5] The crystal structure was converted into a triclinic model in space group $P1$, the carboxylate capped clusters were slightly rotated around c axis and the azo-functionality was manually inserted into this model. Indeed the model exhibited the observed space group symmetry $P6_3/m$. It was energetically optimized by force-field calculations using the forcite routine implemented in Materials Studio. Subsequently the model was refined by Rietveld methods. Residual electron density as identified by Fourier synthesis was attributed to partially occupied oxygen atoms, which serve as dummies for any kind of guest molecules. The linker molecule was refined as fragmented rigid body, i.e. two half molecules split at the azo-group. All other atoms were freely refined. The temperature factors were refined as one parameter for all atoms and a preferred orientation along (110) was also taken into account. The final plot is shown in Fig. S4.1. For Zr-CAU-39 the PXRD data proves its isoreticularity and the cell parameters were refined by the Le Bail method. However, the structure could not be refined by Rietveld methods, which we tentatively attribute to a possible stronger stacking disorder which affects the peak intensities.

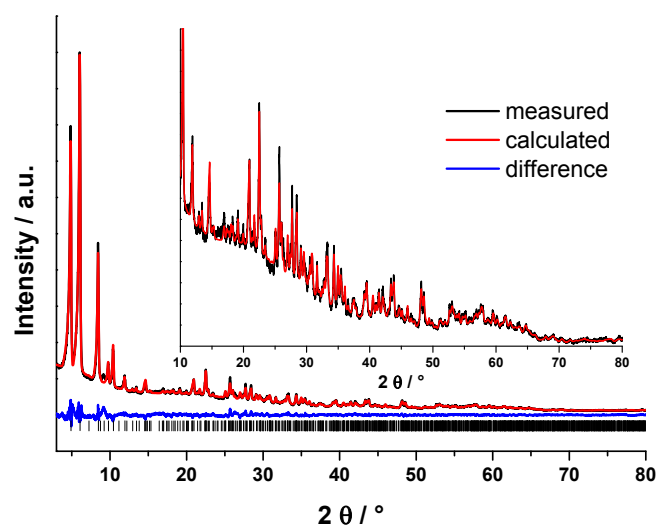


Figure S4.1. Rietveld plot for the final refinement of Hf-CAU-39. Black line gives the experimental data, red line the calculated fit and the blue line is the difference curve. Black bars indicate the Bragg reflection positions.

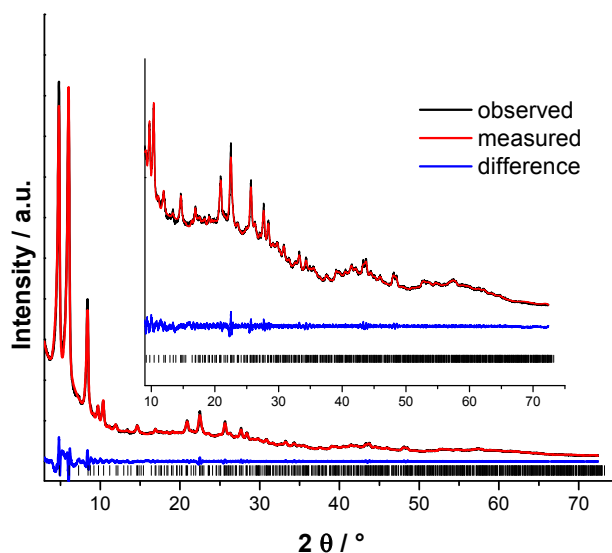


Figure S4.2. Le-Bail-Fit of Zr-CAU-39. Black line gives the experimental data, red line the calculated fit and the blue line is the difference curve. Black bars indicate the Bragg reflection positions.

Table S4.1. Crystallographic data for M-CAU-39 with M = Hf (Rietfeld refinement) and M = Zr (Le-Bail-Fit).

Compound	Hf-CAU-39	Zr-CAU-39
Space Group	<i>P63/m</i>	<i>P63/m</i>
Crystal System	Hexagonal	Hexagonal
$a / \text{Å}$	20.8436(8)	20.86(2)
$c / \text{Å}$	24.367(2)	24.25(3)
Wavelength / Å	Cu $K_{\alpha 1}$	Cu $K_{\alpha 1}$
$R_p / \%$	3.8	2.2
$R_{wp} / \%$	5.0	3.0
GoF	2.5	4.9

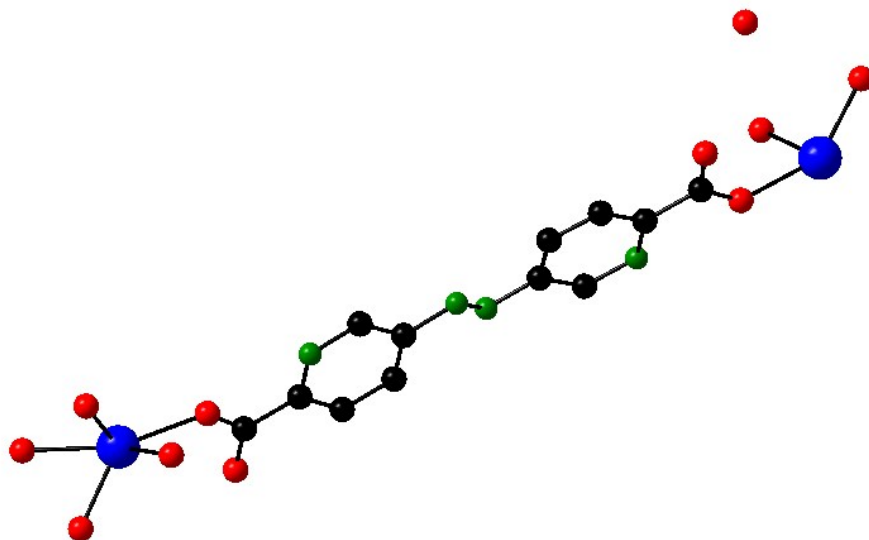


Figure 4.3. Asymmetric unit of M-CAU-39. Oxygen atoms representing water molecules are omitted for clarity.

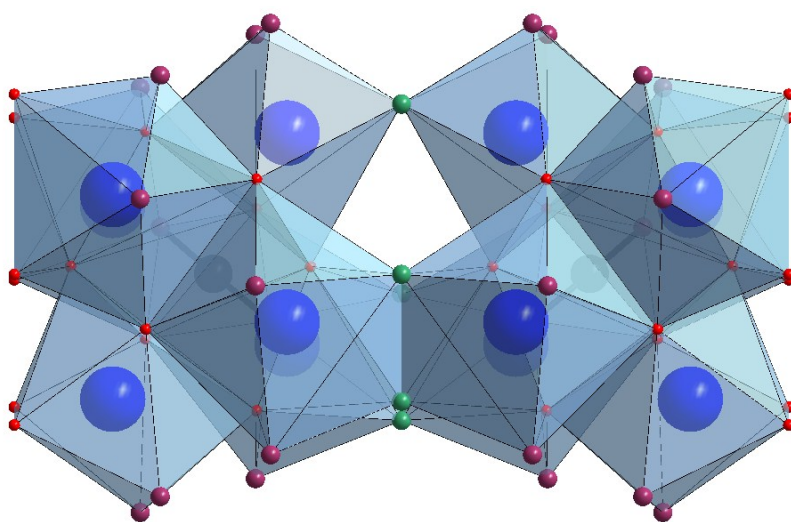


Figure 4.4 The dodecannuclear MO-cluster observed as IBU in the crystal structure of M-CAU-39. The different oxygen atoms are highlighted according the following composition $[M_{12}(\mu_3-O)_8(\mu_3-OH)_8(OH)_6(\mu-OH)_6(H_2O)_6(COO-R)_6]$.

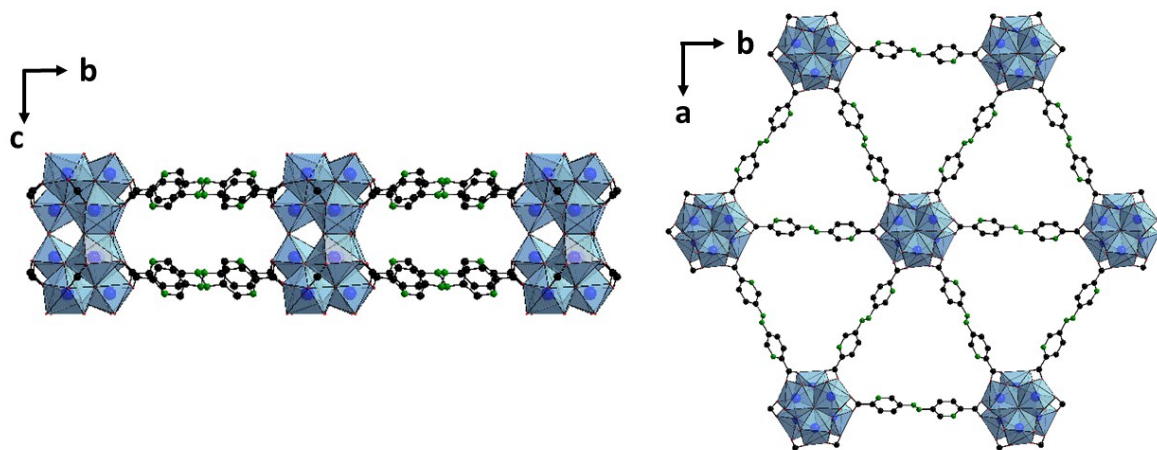


Figure 4.5. One layer of M-CAU-39 along the a -axis (left) and along the c -axis (right)

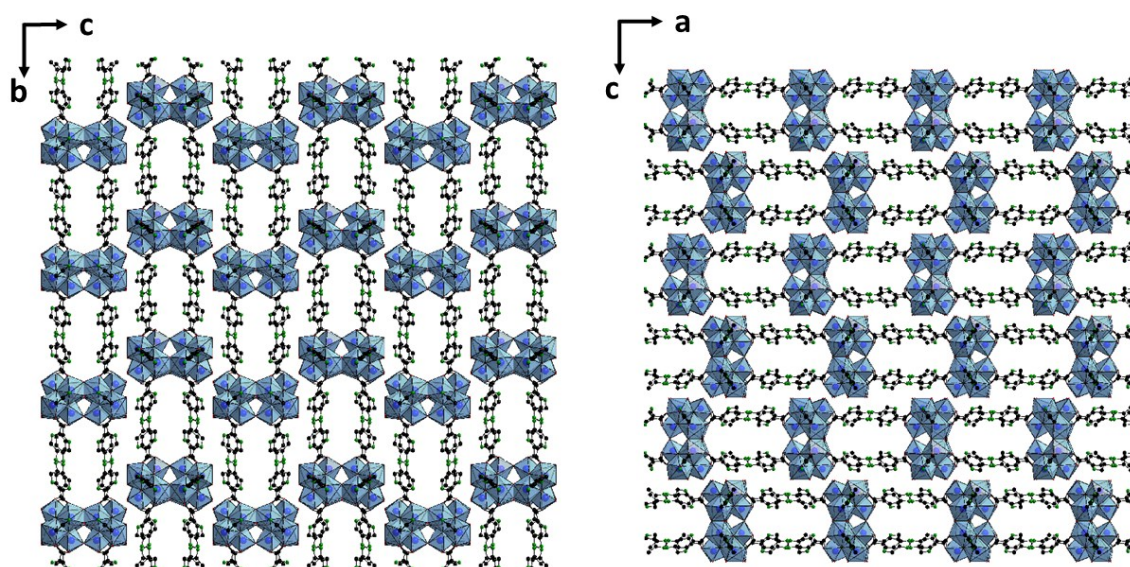


Figure 4.6. Multiple-layers of M-CAU-39 indicating an ABA stacking as seen along the a -axis (left) and along the b -axis (right).

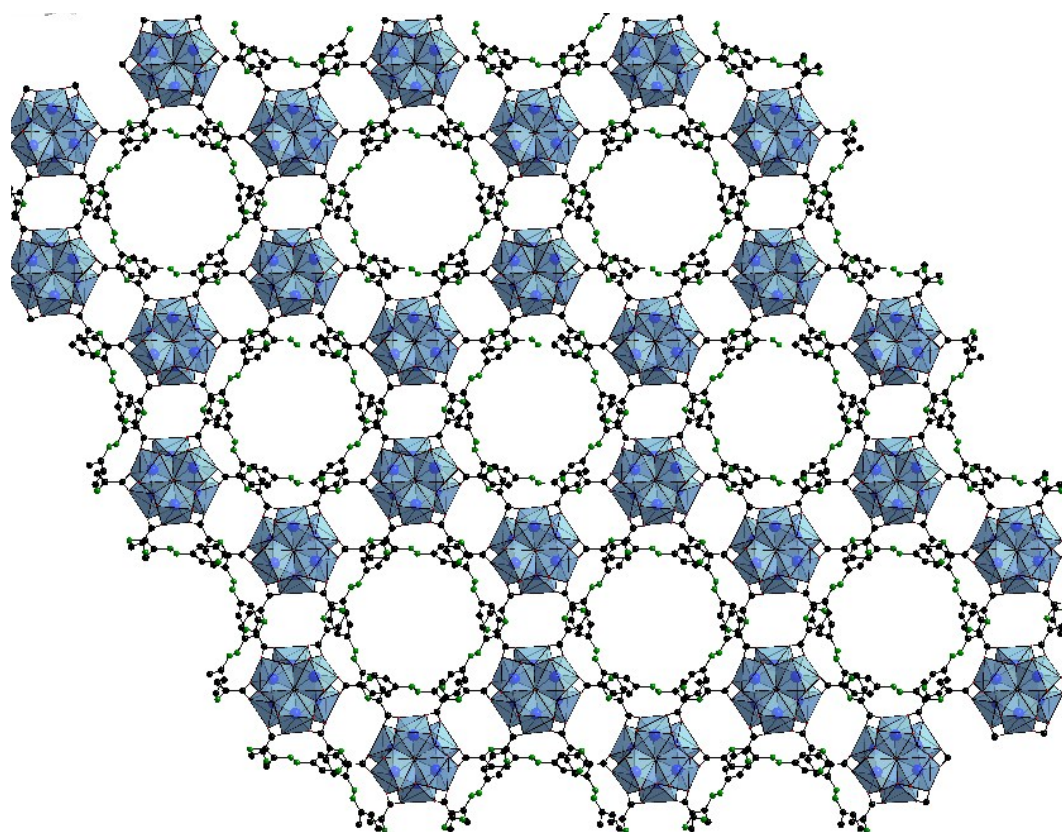


Figure 4.7. Structure of M-CAU-39 as seen along the *c*-axis.

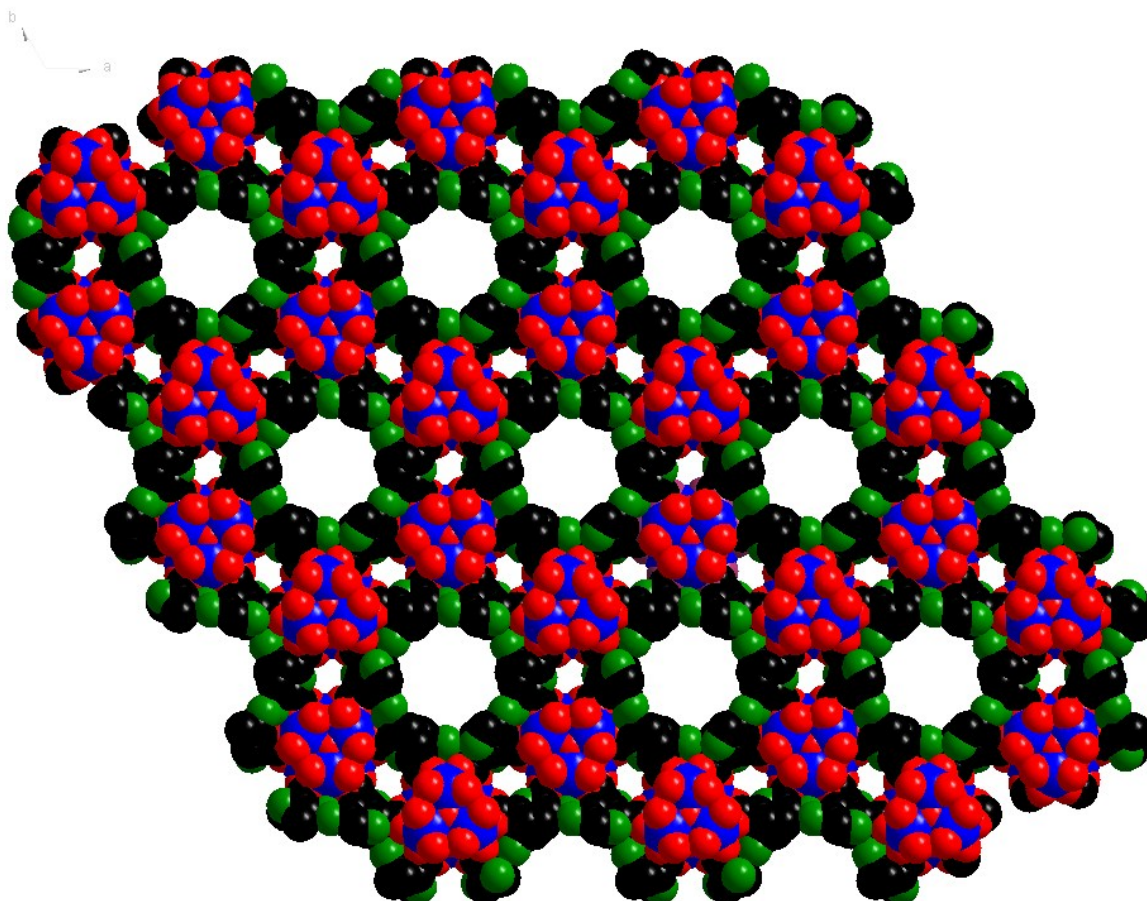


Figure 4.8. Structure of M-CAU-39 as seen along the *c*-axis with a space filling model. The pore diameter is approximately 8 Å.

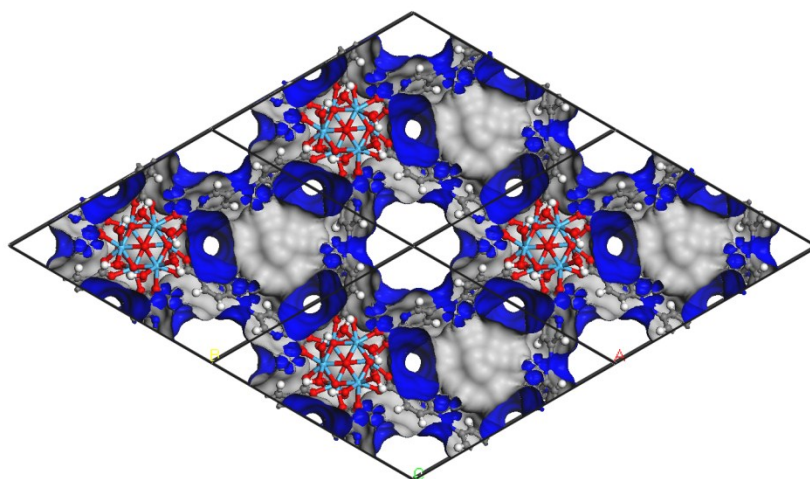


Fig. 4.9. Conolly surface area generated with water as probe molecule.

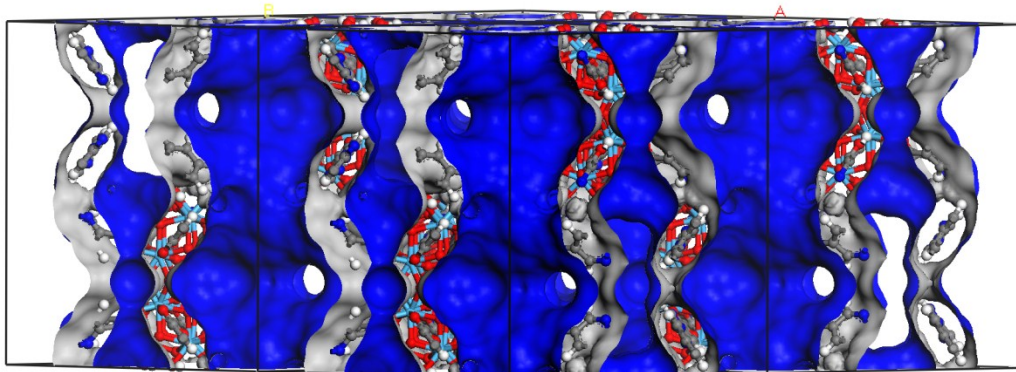


Fig. 4.10. Conolly surface area of the channels seen along $[1\ 1\ 0]$.

S5 M-CAU-39: Thermal stability

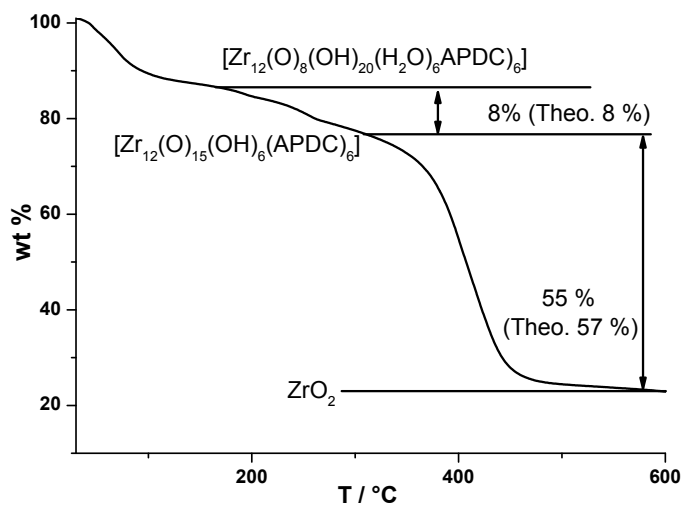


Figure S5.1. TGA plot for Zr-CAU-39 $[\text{Zr}_{12}(\text{O})_8(\text{OH})_{20}(\text{H}_2\text{O})_6(\text{APDC})_6] \cdot x$ solvent showing the weight loss event occurring on dehydration, assigned to the loss of physisorbed water molecules up to 170 °C, above this temperature the dehydration of the dodecancluster (8 wt.%, expected 8 %) is observed, above 320 °C the total structure decompose (55 wt.%; expected 57%).

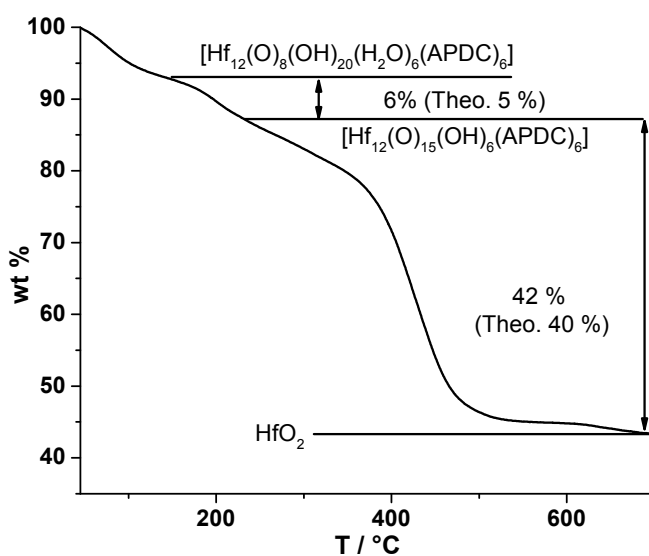


Figure S5.2. TGA plot for Hf-CAU-39 $[\text{Hf}_{12}(\text{O})_8(\text{OH})_{20}(\text{H}_2\text{O})_6(\text{APDC})_6] \cdot x$ solvent showing the weight loss event occurring on dehydration, assigned to the loss of physisorbed water molecules up to 170 °C, above this temperature the dehydration of the dodecancluster (6 wt.%, expected 5 %) is observed, above 320 °C the total structure decompose (42 wt.%; expected 40%).

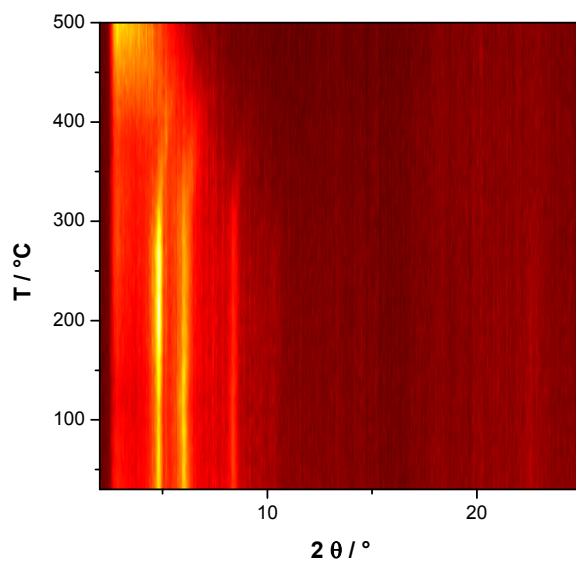


Figure S5.3. VT-PXRD measurement of Zr-CAU-39 measured in transmission geometry using Cu K α 1 radiation. The compound is thermally stable up to approximately 350 °C.

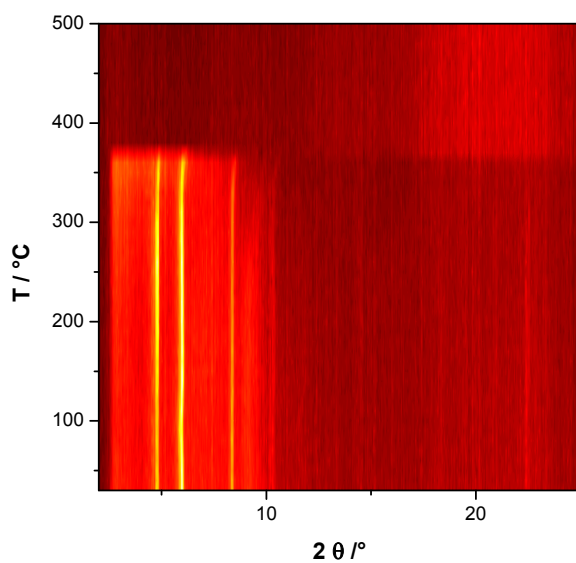


Figure S5.4. VT-PXRD measurement of Hf-CAU-39 measured in transmission geometry using Cu K α 1 radiation. The compound is thermally stable up to approximately 375 °C.

S6 M-CAU-39: Infrared Spectroscopy

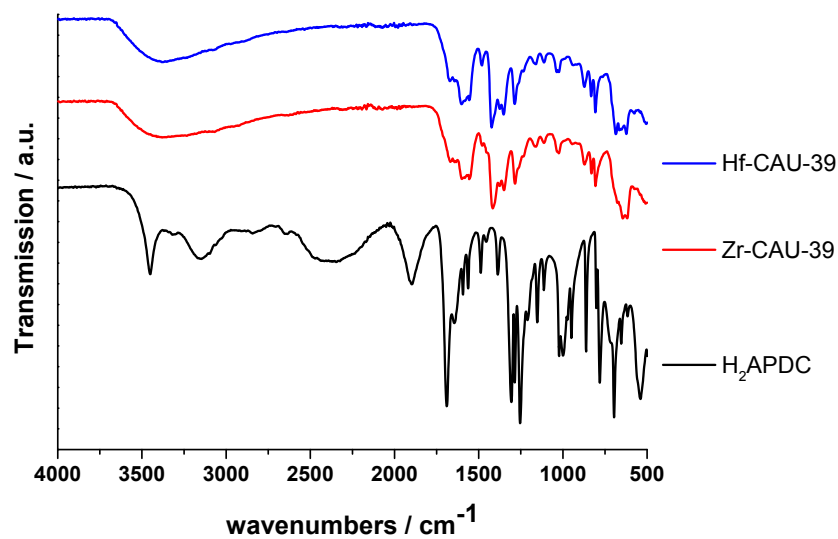


Figure S6.1. FTIR spectrum of M-CAU-39 with M = Zr and Hf.

Tab. S6.1 Classification of the vibrations of M-CAU-39 with M = Zr and Hf from the FTIR spectrum.

	Vibration	Intensity	Wavenumber / cm^{-1}
Zr-CAU-39	OH-stretch – H_2O	b	3434
	Asymmetric CO_2^- stretch – APDC^{2-}	m	1600
	Symmetric CO_2^- stretch – APDC^{2-}	m	1419
Hf-CAU-39	OH-stretch – H_2O	b	3371
	Asymmetric CO_2^- stretch – APDC^{2-}	m	1604
	Symmetric CO_2^- stretch – APDC^{2-}	m	1436

S7 M-CAU-39: N₂ Sorption Experiments

M-CAU-39 with M = Zr and Hf was activated for sorption measurements by heating the sample to 120°C under vacuum overnight. M-CAU-39 is porous towards N₂ at -196 °C (Fig. S7.1).

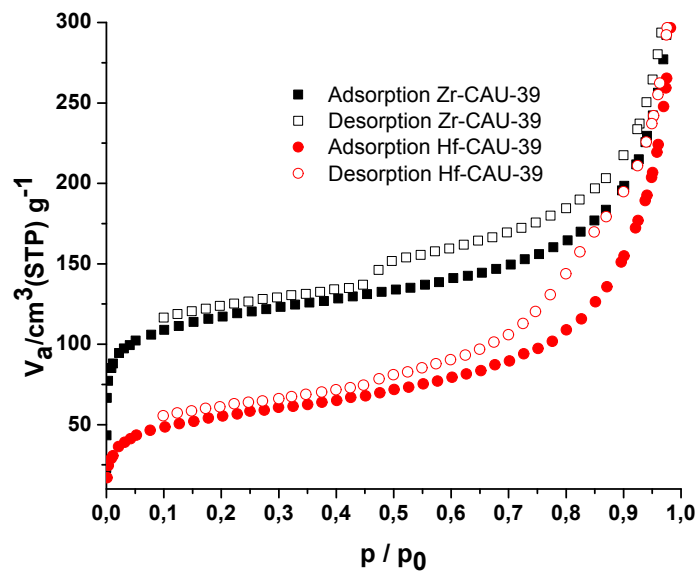


Figure S7.1. N₂-adsorption and desorption isotherms for M-CAU-39 with M = Hf (red) and Zr (black) measured at -196 °C.

Tab. S7.1 The specific surface area ($a_{s,BET}$) and the micropore volume ($V_{mic.}$) based on N₂ adsorption of M-CAU-39 with M = Zr and Hf.

	$a_{s,BET} / \text{m}^2 \cdot \text{g}^{-1}$	$V_{mic.} / \text{cm}^3 \cdot \text{g}^{-1}$
Zr-CAU-39	430	0.21
Hf-CAU-39	200	0.11

S8 References

1. S. Ameerunisha, P. S. Zacharias, *J. Chem. Soc. Perkin. Trans. 2*, **1995**, 1679 – 1682.
2. S. Waitschat, H. Reinsch, N. Stock, *Chem. Commun.*, **2016**, 52, 12698 - 12701.
3. Coelho, *TOPAS-Academic v5*, Coelho Software, Brisbane, Australia, 2012.
4. M. J. Cliffe, E. Castillo-Martinez, Y. Wu, J. Lee, A. C. Forse, F. C. N. Firth, P. Z. Moghadam, D. Fairen-Jimenez, M. W. Gaultois, J. A. Hill, O. V. Magdysyuk, B. Slater, A. L. Goodwin and C. P. Grey, *J. Am. Chem. Soc.*, 2017, **139 (15)**, 5397 - 5404.
5. Materials Studio Version 5.0; Accelrys Inc.: San Diego, **2009**.